THE MOMENTUM DISTRIBUTION OF ^{4}HE AT NON-ZERO TEMPERATURE

D. M. Ceperley
National Center for Supercomputing Applications
Dept. of Physics
University of Illinois at Urbana-Champaign
Champaign, Il. 61820, USA

Path Integral Monte Carlo calculations provide a rigorous way of calculating equilibrium properties of boson systems at finite temperature. The only significant limitation is that the simulations are of a finite system of bosons, typically on the order of 100 atoms. Most results[1,2] have concerned liquid and solid ^{4}He. The method is based on the Feynman-Kac path integral expression[3] for the many body density matrix:

$$\rho(R,R';\beta) = \frac{1}{N!}\sum_P \int dR(t)\ \exp\left[\int_0^\beta -dt'V(R(t'))\right] \qquad (1)$$

where the integral is over all Brownian paths from R to PR', $\beta=1/kT$, R and R' are two sets of the 3N atomic positions, V(R) is potential energy function and PR' is a permutation (relabeling) of the N atoms. To use the above expression on a computer the "path" is made discrete and accurate approximations[4] are made to the high temperature density matrix. The discrete path and permutation is then sampled with a generalization of the Markov chain algorithm (or Metropolis) Monte Carlo method. A sufficiently long sample of the coordinates will then allow one to compute exact properties of the density matrix.

Fig. (1) shows a schematic picture of a typical configuration. Each circle represents an atom, the dark line connecting the dots is the path. The atoms not connected with any other atoms are permuting with themselves and thus "distinguishable". Figure (1) shows a multiply connected region similar to the interior of a torus. For such a region, it is possible to define the superfluid density[5] in terms of the average number of paths which wind around the torus; one is shown in this picture. Others are shown which do not wind and thus do not contribute to superfluidity. The probability of permuting with a nearby atom becomes large at low temperature. The superfluid transition is thus a kind of percolation transition. Comparison with experiment shows good agreement on the computed superfluid density.

The momentum distribution is the Fourier transform[6] of the single particle off-diagonal density matrix, n(r). All this means is that the path of one particle is not required to return to its starting point. One such path is shown in Fig. (1). At high temperatures, where exchange is not important, the two ends remain close to each other; with an average square distance of $1.5\ \hbar^2/mT$. In the superfluid phase the two ends can get arbitrarily far from each other by hooking onto a macroscopically long path. The condensate fraction (probability that a given atom has exactly zero momentum) equals the probability density that the two ends are far apart divided by

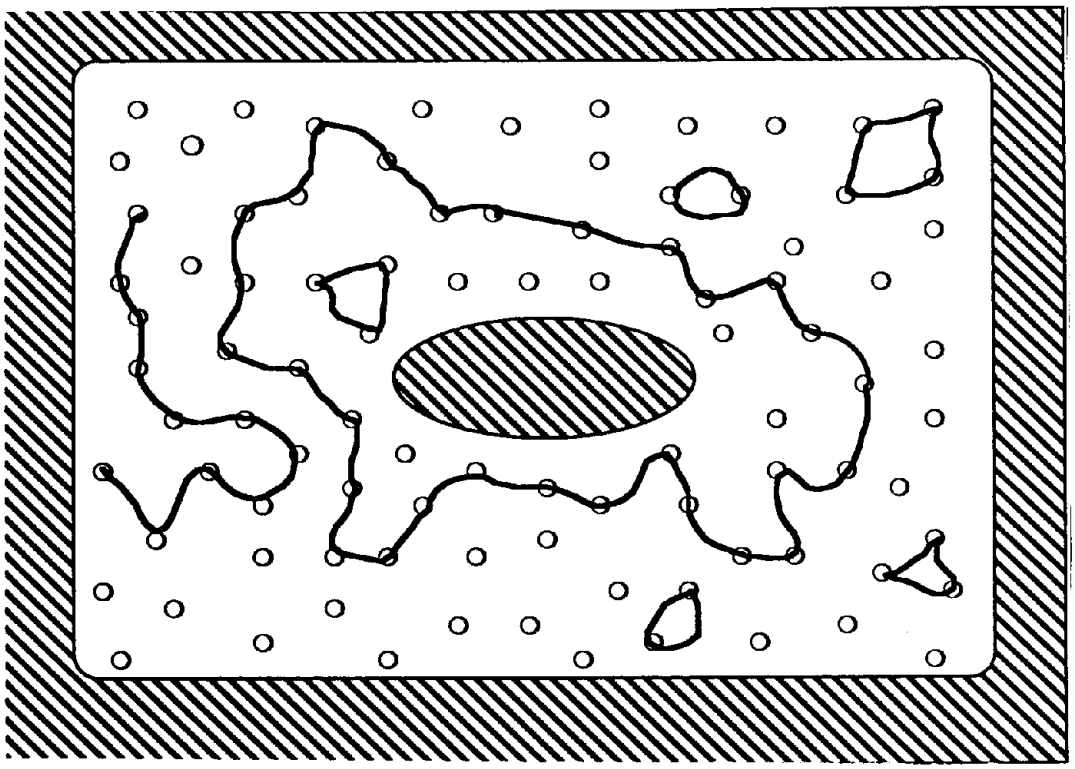

Figure 1: Schematic of a path in liquid helium. The shaded region represents the walls of the container, the circles the helium atoms, and the lines the exchanging paths. The paths of atoms not exchanging are not shown. The path encircling the hole in the container is responsible for superfluidity. The single particle density matrix and the momentum distribution are calculated by determining the end-to-end distribution of the path with two disconnected ends.

the density that they are close together. Thus the condensate fraction and the superfluid density are intimately related. However, they are not the same. In three dimensional liquid helium the condensate fraction is non-zero only when the superfluid fraction is non-zero. Helium films never have a condensate but can become superfluid.

The detailed procedures for the calculation of the momentum distribution are discussed in Ref. (2). Since that article was written we have done additional calculations of the momentum distribution of ^{4}He which we will now summarize.

CALCULATION OF J(y).

In Ref. (2) the momentum distribution of liquid helium at SVP from 1.2K to 3.3K is tabulated. However, what is measured by neutron scattering at high momentum transfers, assuming y-scaling holds, is closely related to the one dimensional momentum distribution, J(y), defined as the probability that an atom has a component of momentum in one direction equal to y. It is easily seen that this is the cosine transform of thesingle particle density matrix.

$$J(y) = 1/\pi \int_0^\infty dr \cos(ry)\, n(r) \qquad (2)$$

It is desirable to compare theory and experiment for J(y) rather than n(k) because the statistical error is smaller for J(y) than n(k) for results obtained both with computer simulations and from neutron scattering. To calculate n(k) from n(r) involves a 3 dimensional fourier transform which has a phase space factor r^2dr. This accentuates the large r statistical fluctuations. In principle, J(y) is obtainable from the n(k)'s in ref.(2) by the use of Fourier transforms and some extra assumptions about the large k behavior of n(k). It is preferable to go back to the original computer simulation data for n(r) and extract J(y) with Eq.(2).

Those results are given in Table 1 along with the computed condensate fraction and kinetic energy (in K). Of course, J(y) should be non-negative for all values of y. The occasional negative entry in Table 1 is a consequence of statistical fluctuations in n(r). This indicates that the results are not very reliable for y greater than about 3 A^{-1}, thus one cannot say much about the exponential behavior of the momentum distribution at large momenta.

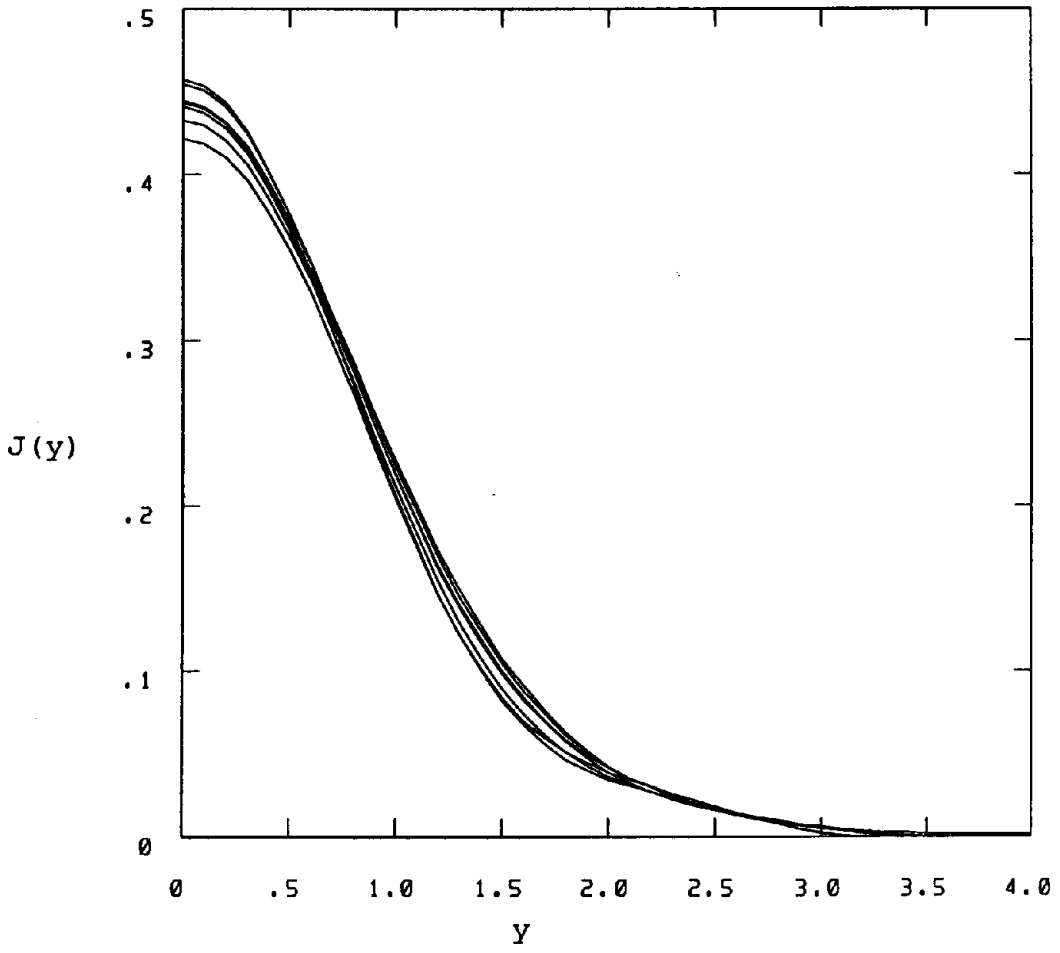

Figure 2: J (in A) versus y (in A^{-1}) in liquid helium along SVP. The density is about $0.022/A^3$ and the temperatures range from 1.2K to 4K.

Fig. (2) shows the computed J(y) along the SVP line from 1.18K to 4K. The assumption often made, that the non-condensed

Table 1: J(y) in liquid and solid helium.

state	bcc ⇔ fcc		nf	nf	sf	sf	sf	sf	sf	nf	nf	sf	sf	nf
T (K)	1.60	1.67	2.35	4.00	1.18	1.54	1.82	2.22	2.50	3.33	4.00	1.18	2.00	4.00
dens.	0.0288	0.0288	0.0288	0.0288	0.0218	0.0218	0.0219	0.0220	0.0218	0.0207	0.0207	0.0260	0.0260	0.0260
cond.	0.0000	0.0000	0.0002	0.0000	0.0687	0.0873	0.0634	0.0272	0.0131	0.0040	0.0017	0.0262	0.0120	0.0003
kin. energy	24.40	24.08	24.75	25.66	14.17	14.35	14.71	15.92	15.91	16.00	16.93	19.11	20.11	21.81
y(1/A)							J(y)							
0.0	0.3544	0.3579	0.3577	0.3502	0.4400	0.4212	0.4319	0.4428	0.4571	0.4542	0.4436	0.3913	0.3954	0.3837
0.1	0.3529	0.3564	0.3561	0.3487	0.4368	0.4184	0.4289	0.4395	0.4535	0.4507	0.4405	0.3893	0.3933	0.3817
0.2	0.3485	0.3519	0.3515	0.3444	0.4275	0.4101	0.4201	0.4299	0.4428	0.4404	0.4312	0.3834	0.3870	0.3757
0.3	0.3413	0.3444	0.3439	0.3373	0.4122	0.3965	0.4058	0.4145	0.4256	0.4238	0.4162	0.3738	0.3767	0.3660
0.4	0.3314	0.3343	0.3335	0.3276	0.3916	0.3780	0.3864	0.3939	0.4029	0.4020	0.3964	0.3607	0.3628	0.3529
0.5	0.3193	0.3217	0.3208	0.3156	0.3665	0.3551	0.3628	0.3691	0.3759	0.3760	0.3725	0.3444	0.3456	0.3371
0.6	0.3050	0.3070	0.3060	0.3016	0.3376	0.3284	0.3357	0.3412	0.3459	0.3471	0.3456	0.3253	0.3257	0.3189
0.7	0.2891	0.2906	0.2895	0.2860	0.3061	0.2990	0.3061	0.3112	0.3140	0.3165	0.3167	0.3040	0.3037	0.2990
0.8	0.2718	0.2728	0.2717	0.2690	0.2730	0.2678	0.2750	0.2804	0.2816	0.2852	0.2869	0.2810	0.2802	0.2779
0.9	0.2535	0.2540	0.2530	0.2511	0.2396	0.2358	0.2434	0.2495	0.2495	0.2542	0.2570	0.2569	0.2557	0.2561
1.0	0.2346	0.2347	0.2338	0.2327	0.2069	0.2043	0.2123	0.2196	0.2186	0.2243	0.2278	0.2323	0.2310	0.2340
1.1	0.2155	0.2151	0.2144	0.2141	0.1758	0.1742	0.1825	0.1911	0.1895	0.1960	0.1998	0.2077	0.2066	0.2121
1.2	0.1965	0.1957	0.1952	0.1955	0.1473	0.1465	0.1548	0.1647	0.1627	0.1696	0.1736	0.1838	0.1830	0.1906
1.3	0.1779	0.1767	0.1764	0.1774	0.1219	0.1219	0.1298	0.1406	0.1384	0.1455	0.1495	0.1609	0.1607	0.1699
1.4	0.1599	0.1584	0.1582	0.1598	0.1000	0.1008	0.1077	0.1189	0.1169	0.1237	0.1275	0.1394	0.1401	0.1502
1.5	0.1428	0.1410	0.1409	0.1431	0.0817	0.0833	0.0888	0.0998	0.0981	0.1045	0.1079	0.1198	0.1213	0.1318
1.6	0.1266	0.1247	0.1246	0.1273	0.0668	0.0694	0.0731	0.0833	0.0821	0.0876	0.0906	0.1021	0.1044	0.1148
1.7	0.1116	0.1095	0.1094	0.1125	0.0552	0.0585	0.0603	0.0690	0.0687	0.0732	0.0755	0.0865	0.0896	0.0993
1.8	0.0977	0.0956	0.0954	0.0989	0.0462	0.0502	0.0502	0.0570	0.0576	0.0610	0.0627	0.0729	0.0766	0.0855
1.9	0.0851	0.0830	0.0827	0.0865	0.0394	0.0439	0.0422	0.0471	0.0486	0.0508	0.0518	0.0612	0.0654	0.0732
2.0	0.0736	0.0716	0.0712	0.0752	0.0342	0.0388	0.0360	0.0388	0.0413	0.0423	0.0428	0.0512	0.0558	0.0624
2.1	0.0634	0.0615	0.0610	0.0650	0.0300	0.0344	0.0310	0.0321	0.0353	0.0354	0.0353	0.0427	0.0474	0.0531
2.2	0.0543	0.0526	0.0520	0.0560	0.0266	0.0303	0.0268	0.0267	0.0303	0.0296	0.0292	0.0355	0.0402	0.0449
2.3	0.0462	0.0448	0.0442	0.0480	0.0235	0.0263	0.0231	0.0222	0.0259	0.0247	0.0242	0.0292	0.0340	0.0379
2.4	0.0392	0.0380	0.0374	0.0409	0.0206	0.0222	0.0196	0.0186	0.0220	0.0205	0.0201	0.0238	0.0285	0.0319
2.5	0.0331	0.0321	0.0316	0.0348	0.0178	0.0180	0.0162	0.0155	0.0185	0.0168	0.0167	0.0189	0.0237	0.0267
2.6	0.0278	0.0270	0.0267	0.0295	0.0150	0.0140	0.0130	0.0129	0.0153	0.0136	0.0139	0.0147	0.0196	0.0223
2.7	0.0232	0.0227	0.0226	0.0248	0.0124	0.0103	0.0099	0.0107	0.0123	0.0108	0.0115	0.0110	0.0160	0.0185
2.8	0.0193	0.0190	0.0191	0.0209	0.0098	0.0070	0.0071	0.0087	0.0097	0.0084	0.0094	0.0079	0.0129	0.0154
2.9	0.0160	0.0159	0.0161	0.0175	0.0075	0.0044	0.0046	0.0070	0.0075	0.0064	0.0076	0.0055	0.0104	0.0127
3.0	0.0132	0.0133	0.0137	0.0146	0.0055	0.0023	0.0026	0.0055	0.0056	0.0048	0.0062	0.0037	0.0082	0.0105
3.1	0.0108	0.0111	0.0117	0.0122	0.0037	0.0009	0.0012	0.0044	0.0041	0.0034	0.0049	0.0027	0.0065	0.0087
3.2	0.0088	0.0092	0.0100	0.0101	0.0021	0.0000	0.0002	0.0035	0.0028	0.0024	0.0039	0.0022	0.0051	0.0071
3.3	0.0071	0.0077	0.0085	0.0084	0.0008	-0.0005	-0.0003	0.0028	0.0018	0.0016	0.0032	0.0022	0.0040	0.0059
3.4	0.0058	0.0063	0.0073	0.0069	-0.0003	-0.0008	-0.0004	0.0025	0.0010	0.0009	0.0025	0.0026	0.0032	0.0048
3.5	0.0046	0.0052	0.0063	0.0057	-0.0013	-0.0009	-0.0002	0.0023	0.0003	0.0003	0.0021	0.0030	0.0025	0.0039
3.6	0.0036	0.0043	0.0054	0.0047	-0.0020	-0.0010	0.0000	0.0022	-0.0003	-0.0002	0.0017	0.0035	0.0019	0.0031
3.7	0.0029	0.0035	0.0047	0.0039	-0.0026	-0.0011	0.0002	0.0022	-0.0008	-0.0006	0.0014	0.0039	0.0014	0.0025
3.8	0.0022	0.0029	0.0040	0.0032	-0.0030	-0.0013	0.0003	0.0022	-0.0011	-0.0009	0.0011	0.0040	0.0011	0.0020
3.9	0.0017	0.0023	0.0034	0.0026	-0.0031	-0.0014	0.0004	0.0020	-0.0012	-0.0011	0.0009	0.0040	0.0008	0.0016
4.0	0.0013	0.0018	0.0028	0.0021	-0.0030	-0.0014	0.0003	0.0018	-0.0012	-0.0012	0.0007	0.0039	0.0006	0.0012

part of the momentum distribution is independent of temperature, is approximately correct. Most of the differences between the various J(y)'s seen in Fig. (2) are the result of statistical fluctuations. This is because in performing the cosine transform in Eq. (2) for a superfluid we assume that n(r) equals its asymptotic value, n_o, for $r>R_c$, where R_c is taken to be 5.5 A. Because the assumed value of n_o has statistical fluctuations of the order of $\delta n_o = 0.005$, this procedure will introduce noise in J(y) of the form $\delta n_o \sin(yR_c)/(\pi y)$. Thus, the statistical error in J(y) at small y can be as large as 0.01A, about what is observed in Fig. (2).

DENSITY DEPENDANCE OF THE MOMENTUM DISTRIBUTION.

The data in Table 1 are at three different densities in units of atoms/A^3. The lowest density is very close to SVP where most theoretical and experimental studies have been carried out. The intermediate density, 0.02596/A is near the liquid-solid transition at zero temperature. Fig.(3) shows J(y)

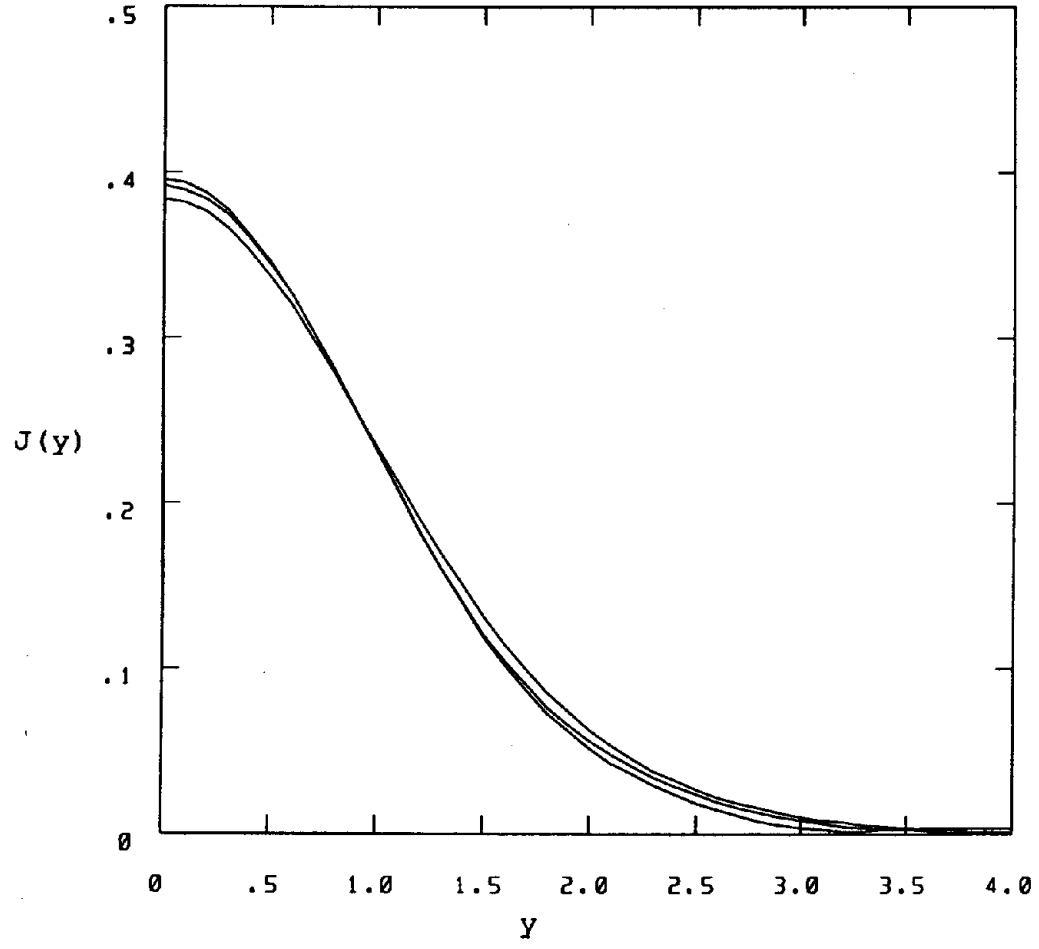

Figure 3: J (in A) versus Y (in A^{-1}) for liquid helium at a density of 0.026/A^3 and temperature from 1.2K to 4K.

at the higher density. It is seen that the curves at low and high density are quite similar. The main effect is that the zero-temperature kinetic energy has increased from 14.2K to 19.1K. The condensate fraction drops from 8% at SVP to 3%.

This is in agreement with GFMC calculations[7] but not with neutron scattering experiments of Sokol.[8] Finally, Table 1 contains J(y) for an even higher density which cuts through the liquid-solid line.

VARIATION OF THE MOMENTUM DISTRIBUTION FROM LIQUID TO SOLID

At a higher density, we have computed the momentum distribution in both the liquid and solid phase (both a fcc structure and a bcc structure). The results are given in Table 1. Fig. (4) compares the J(y)'s from these calculations It is seen that the momentum distribution is very insensitive to whether the system is in a liquid or solid phase, less sensitive than the pair correlation function, for example. Neutron scattering measurements at the same density and temperature also show this independence with respect to the phase[9]. The momentum distribution is controlled by the cage surrounding an atom and the local environment does not change much when going from a normal liquid to a solid. That is controlled mainly by the density. We have not looked for angular dependance of the momentum distribution in the solid phase.

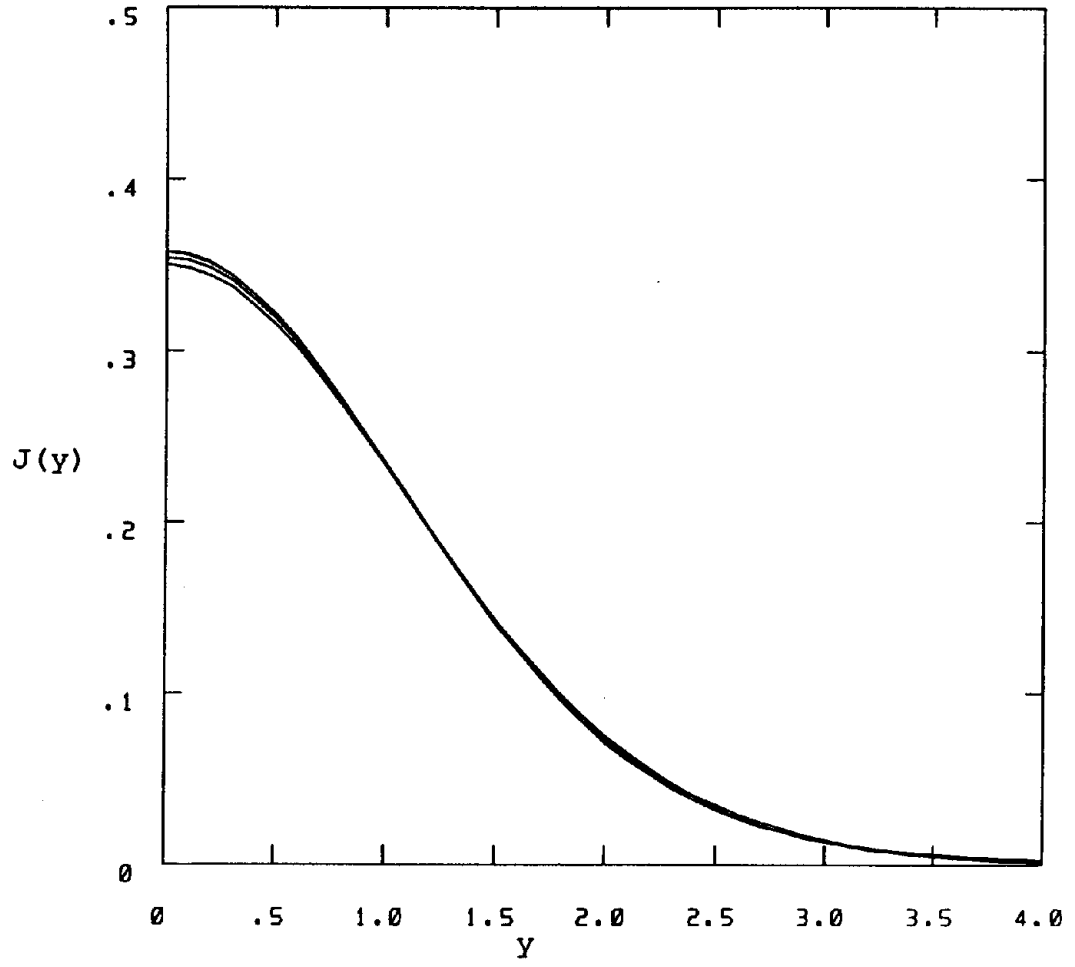

Figure 4: J (in A) versus y (in A^{-1}) for liquid and solid helium at a density of $0.0288/A^3$ and temperatures from 1.6K to 4K.

EFFECT OF DIMENSIONALITY ON THE MOMENTUM DISTRIBUTION.

The theoretical description of superfluidity in two dimensional He films is given by the theory of Kosterlitz and Thouless, rather than by the macroscopic occupation of the zero momentum state as it is bulk (3 dimensional) He. According to this theory the end-to-end distribution of the polymer in Fig. (1), n(r), decays algebraically to zero at all finite temperatures, if the system is superfluid:

$$n(r) = n_o (d/r)^{-\eta} \quad \text{where } \eta = mkT/2\pi h^2\rho \qquad (3)$$

The exponent η goes to zero linearly with the temperature; thus n_o is the 2 dimensional analogue of the condensate fraction. Ref. (10) contains the results of path integral calculations in the zero pressure liquid. In that paper, it was determined that 2 dimensional He films will become superfluid below 0.72K, and that $n_o = 0.22$ and $d = 3.7$ A. This value of n_o is similar to the results of Green's Function Monte Carlo calculations[11]. The parameter d has the interpretation in the Kosterlitz-Thouless theory of the vortex core size.

In Fourier transforming to get J(y) one arrives at a singular behavior at small momentum, not a delta function:

$$J(y) \approx y^{\eta-1} \qquad (4)$$

The difference in the path integral simulations between the behavior in two and three dimensions is very noticeable. However experimentally it is not clear whether there will be such a pronounced effect of the dimensionality after the distribution function is broadened by instrumental and final state effects.

TWO BODY OFF-DIAGONAL DENSITY MATRIX.

The experimental search by neutron scattering for the momentum condensate actually measures the density-density response function, $S(k,\omega)$. At very high momentum transfers $S(k,\omega)$ can be calculated with the aid of the impulse approximation and becomes proportional to the momentum distribution. However, $S(k,\omega)$ converges exceedingly slowly to this limit. Agreement between experiment and theory is only obtained with the use of more accurate expressions for these final state effects. For a detailed discussion see other contributions in this volume and their references. One of the major inputs to the final state effect calculations is the probability that a spectator atom carries off some of the momentum of the neutron which is proportional to the expectation value of

$$\sum_n a^\dagger_{k+q}\, a^\dagger_{n-q}\, a_n\, a_k \qquad (5)$$

where a and $a^\dagger$ are destruction and creation operators in momentum space. The Fourier transform of this operator can be written in coordinate space as the probability distribution that the two ends of the polymer are at positions $\mathbf{r}_1$ and $\mathbf{r}_1'$ and one

other atom is at position $\mathbf{r}_2$. Let us define $n_2(\mathbf{r}_1,\mathbf{r}_1',\mathbf{r}_2;\beta)$ as that distribution function, normalized so that the integral over $\mathbf{r}_2$ is the single particle off-diagonal density matrix, $n_1(\mathbf{r}_1,\mathbf{r}_1';\beta)$.

We have calculate n_2 with Path Integral Monte Carlo. The full analysis of this function and its consequences for analysis of final state effects in neutron scattering will appear elsewhere. Here we will simply compare to a simple statistical approximation, similar in spirit to the superposition approximation of classical liquids. Let g(r) be the radial distribution function, the average density a distance r from one atom divided by the total density. Then at small and large $\mathbf{r}_1$-$\mathbf{r}_1'$ it is reasonable to write:

$$n_2^A(\mathbf{r}_1,\mathbf{r}_1',\mathbf{r}_2;\beta) = n_1(\mathbf{r}_1,\mathbf{r}_1';\beta)\,[g(\mathbf{r}_2-\mathbf{r}_1)g(\mathbf{r}_2-\mathbf{r}_1')]^{1/2} \quad (6)$$

To compare n_2 with n_2^A we have fixed the end-to-end distance of the polymer, $\mathbf{r}_1$-$\mathbf{r}_1'$, at 4 A and averaged over the angle between $\mathbf{r}_1$-$\mathbf{r}_1'$ and $\mathbf{r}_1$-$\mathbf{r}_2$. Shown in Fig. (5) are the approximate result

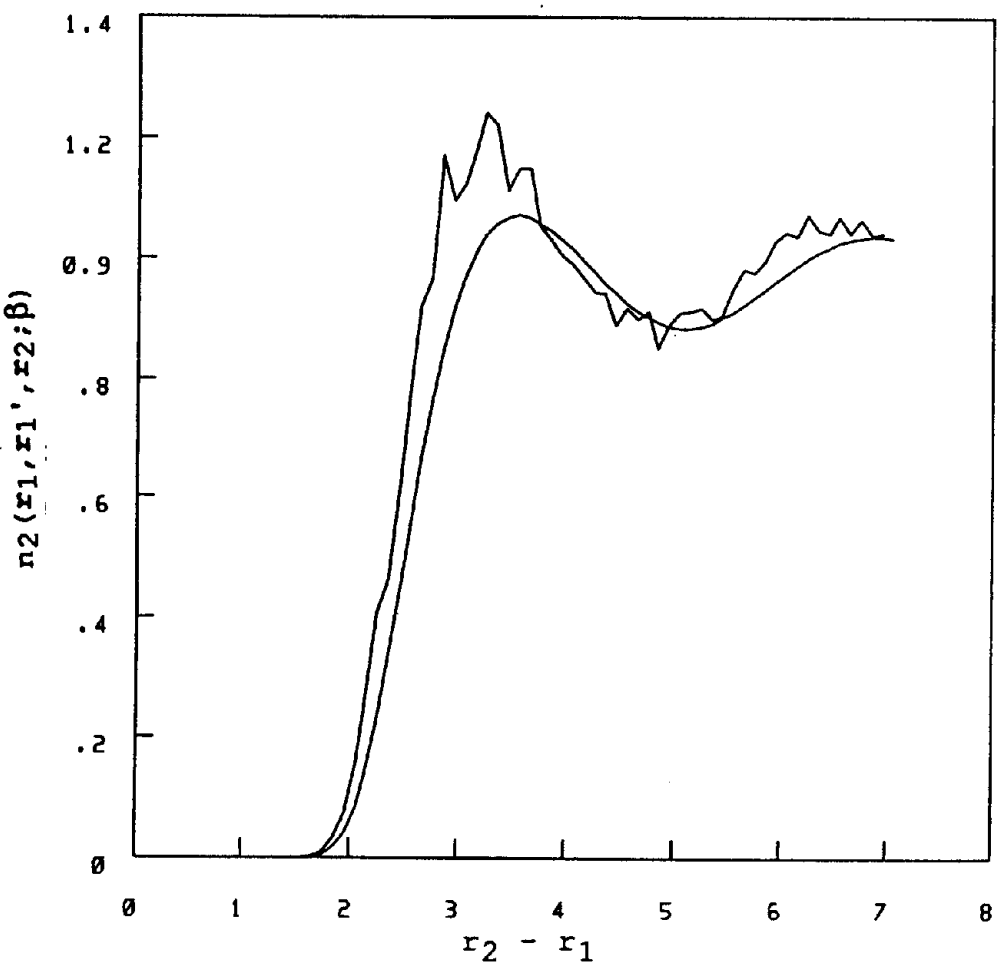

Figure 5: The sphericalized two partide density matrix at a density of $0.022/A^3$ and temperature 1.2K with $r_1 - r_1' = 4A$. The upper curve with noise is the result of PIMC. The smooth curve is the result of Eq. (6).

(the curve without noise) and the exact result (with statistical noise) for the spherical average of n_2 around $\mathbf{r}_1$ at a temperature of 1.2K and at SVP. The approximation is fairly accurate except at the first peak where it is too small by about 10%. Similar results are obtained at other values of $\mathbf{r}_1$-$\mathbf{r}_1'$ and at other temperatures.

CONCLUSIONS.

The path integral method is able to calculate quite accurate momentum distributions for bose systems at finite temperature. At the present time there are no significant discrepancies with respect to experiment.

ACKNOWLEDGEMENTS

The simulations of helium films were done in collaboration with E. L. Pollock. The calculations of n_2 and the momentum distribution at high density were supported by a grant of computer time on the CRAY-X/MP at the National Resource for Supercomputing Applications, University of Illinois Urbana-Champaign.

REFERENCES

1. D. M. Ceperley and E. L. Pollock, Phys. Rev. Letts. **56**,351 (1986),
2. D. M. Ceperley and E. L. Pollock Can. J. of Physics,**65**,1416 (1987).
3. R. P. Feynman, Statistical Mechanics (Benjamin, Reading, Mass. 1972).
4. E. L. Pollock and D. M. Ceperley, Phys. Rev. **B30**,2555(1984).
5. E. L. Pollock and D. M. Ceperley, Phys. Rev. **B36**,8343(1987).
6. O. Penrose and L. Onsager, Phys. Rev. **104**,576(1956).
7. P. Whitlock, and R. M. Panoff, Can. J. of Phys.**65**,1409(1987).
8. P. Sokol, Can. J. of Phys.**65**,1393(1987).
9. R. O. Simmons, Can. J. of Phys. **65**,1401 (1987).
10. D. M. Ceperley and E. L. Pollock, Phys. Rev.**B**, in press,(1988).
11. R. B. Panoff and P. Whitlock, this volume.